Proton Polarizability of Hydrogen-Bonded Network and its Role in Proton Transfer in Bacteriorhodopsin

Jianping Wang and Mostafa A. El-Sayed*

Laser Dynamics Laboratory, School of Chemistry and Biochemistry, Georgia Institute of Technology, Atlanta, Georgia 30332-0400

Received: December 22, 1999; In Final Form: February 24, 2000

Room-temperature time-resolved step-scan Fourier Transform Infrared (FTIR) spectroscopy has been used to study the photocycle of native bacteriorhodopsin (bR) suspension in both H_2O and D_2O. The kinetics of the retinal isomerization, and that of the protonation/deprotonation of the proton acceptor, Asp85, are compared in the μs to ms time domain. It is found that hydrogen/deuterium (H/D) isotope exchange does not significantly affect the kinetics of the retinal isomerization and relaxation processes. However, the protonation/deprotonation processes of Asp85 COO^- become slower in D_2O. We also studied the kinetics of the continuum absorbance change in the 1850−1800 cm^{-1} frequency region, which has previously been proposed to correspond to the absorption of the delocalized proton that is involved in the proton transport to the surface during the photocycle. An H/D isotope shift of the frequency range of this continuum absorbance has been confirmed by the observation that the band in the 1850−1800 cm^{-1} disappears in the photocycle of bR in D_2O. These results could support the previous proposal that the intramolecular proton release pathway consists of an H-bonded network. Our results also suggest that the two independent processes, the transfer of a proton from the Schiff base to Asp85 and the release of a different proton to the extracellular surface, are closely coupled events.

Introduction

Bacteriorhodopsin (bR), the only protein in the purple membrane (PM) of *Halobacterium salinarium*,[1] has a retinylidene chromophore that binds to the ϵ-amino group Lys216 through a protonated Schiff base and has been known as a light-driven proton pump. The electrochemical gradient generated across the membrane can be used by the cell for ATP synthesis.[2] The primary structure of bR contains only one polypeptide chain of 248 amino acid residues in the form of α-helices.[3] Upon illumination, bR undergoes a cyclic photoreaction with an all-trans to 13-cis retinal isomerization and the translocation of protons from the cytoplasmic to the extracellular side of the membrane.[4] In the photocycle of bR, a series of photointermediates, J, K, L, M, N, and O, have been spectroscopically identified,[4−6] with lifetimes ranging from hundreds of femtoseconds to tens of milliseconds.

Two amino acid residues involved in the proton translocation have been identified by site-directed mutagenesis. Asp85 is the proton acceptor from the protonated Schiff base,[7] and Asp 96 is the proton donor to the Schiff base.[8,9] In the L to M transition, a proton is transferred from the Schiff base to Asp 85, which remains protonated for a few milliseconds. Proton release is detected by pH-sensitive dyes[10,11] bound to the extracellular surface in the tens of microseconds after the initiation of the photocycle. Thus, the proton appearing at the surface is not the proton that is dissociated from the protonated Schiff base. Another proton donor group, XH, must be involved. Possible candidates, such as Glu204 and Arg 82, have been suggested as such a proton-release group, XH.[12,13]

Recently, by using time-resolved FTIR, Rammelsberg et al.[14] have reported that during the L to M transition, Glu204 is found to be protonated and, therefore, less likely to be the proton-release group XH. On the other hand, these authors have found that the IR continuum absorbance in the 1850 and 1800 cm^{-1} frequency region changes on the time scale of proton pumping, and therefore, they have suggested that the intramolecular proton transfer occur via an H-bonded network to the surface of the protein.

In general, the observation of a continuum absorbance indicates the presence of a proton delocalized over an H-bonded chain with large proton polarizability.[15] Proton polarizabilities are caused by fluctuation and shifts of the proton within the H-bonded chain. Particularly, large proton polarizabilities are observed due to the collective motion of the protons within H-bonded chains. Therefore, it is possible to follow the kinetics of the polarizability change of a delocalized proton. Proton polarizabilities are about 2 orders of magnitude greater than the polarizabilities due to distortion of electronic systems. For an H-bonded system, either homoconjugated ($A^-\cdots A$) or heteroconjugated ($A^-\cdots H^+\cdots B$), the direct origin of the intense IR continuum absorbance is the delocalized proton within an H-bonded network. The homoconjugated system gives a symmetrical double minimum proton potential well or a symmetrical broad, flat potential well along the $A\cdots H\cdots A$ coordinate. The continuum absorbance band usually appears in the frequency region between the major modes of H−O−H vibrations in H-bond system.[15]

In the present study, to understand the detailed proton release pathway inside the membrane during bR photocycle, we have carried out the time-resolved FTIR of bR in both H_2O and D_2O. The continuum absorption in the 1850−1800 cm^{-1} range in the μs−ms time domain has been examined. Our results confirm the presence of a bleached continuum band in the region 1850−1800 cm^{-1}, with its kinetics similar to that of the protonation of Asp85 in H_2O, that does not exists in D_2O.

* To whom correspondence should be addressed. Tel: (404) 894-0292. Fax: (404) 894-0294. Email: mostafa.el-sayed@chemistry.gatech.edu.

10.1021/jp994460u CCC: $19.00
Published on Web 03/31/2000

Materials and Methods

bR containing purple membrane fragments were isolated from the *Halobacterium salinarium* strain ET1001 as described previously.[1] The membrane suspension in H_2O or D_2O was prepared by washing the membrane fragments 3−4 times by centrifugation at neutral pH. After centrifugation, the pellet was collected and squeezed between two CaF_2 plates. The optical density of such a bR pellet is ∼1.0 at 570 nm. Samples were kept at 25 °C during experiments.

The step-scan time-resolved FTIR system[16] was an IFS 66/S system (Bruker, Billerica, MA), equipped with a MCT detector (Kolmar Technologies, mode KMPV11, with appropriate preamplifier for both ac- and dc-coupled signal output). The ac-coupled signal was amplified additionally by a factor of 125, using a DC-300 MHz amplifier (Stanford Research Systems, model SR 445), before inputting it to a 200 MHz digitizer. The dc-coupled signal of the detector was first adjusted to remove the offset and then amplified by a factor of 2−5, using a low-noise amplifier (Stanford Research Systems, SR 560), to approach ±1V peak to peak amplitude before introducing it to the digitizer. The dc-coupled signal was used for phase correction when the ac-coupled transient spectra were collected. The MCT detector−preamplifier system gives a linear relationship between the signal output and the IR beam intensity, which guarantees no significant baseline shift in the obtained ac-coupled transient spectra. The dc-coupled single-beam spectra were collected separately. The time-resolved FTIR spectrum for a certain time domain after photoexcitation was calculated based on the ac-coupled transient spectrum and dc-coupled single beam spectrum: $\Delta Abs = \log(ac/dc + 1)$. To cover the time range from μs to ms, two different experiments have been carried out, with a time resolution of either 1 μs or 10 μs and a spectral resolution of 4 cm^{-1}. The spectral window is confined between 750 and 2000 cm^{-1} by using an antireflecting coated germanium band-pass filter. The results were obtained by averaging 10−14 coadditions during the step-scan experiment and 6−9 separate experiments. The bR samples were photoexcited by using the second harmonic output (532 nm) of a Nd:YAG laser (Quantum-Ray, DCR-3) at a repetition rate of 10 Hz and a laser energy of 3 mJ/pulse. All of the measurements were carried out at 25 °C.

Result

Transient Spectra of L/bR and M/bR in H_2O and D_2O. Figure 1 gives the transient FTIR spectra of bR in H_2O and D_2O, obtained at delay times of 8 μs (L/bR, spectra a and b) and 100 μs (M/bR, spectra c and d). In the time-resolved difference spectra, the positive bands belong to the photocycle intermediates and the negative bands belong to the ground state (bR_{568}). bR, in either H_2O or D_2O, has a complete photocycle and functions as a proton or a deuteron pump. The top two are typical features of L/bR difference spectra, whereas the bottom two are typical features of M/bR difference spectra. The fingerprint region of retinal is also shown at 1528 cm^{-1} for the C═C stretch mode and 1256, 1200, and 1166 cm^{-1} for the C−C stretch modes. From the L to M transition, it is clear that protonated aspartate groups that give a negative band at 1740 cm^{-1}, upon L formation in H_2O, disappear when M is formed. The positive band at 1186 cm^{-1} is a distinct feature for the formation of L, due to the C−C stretching mode of the C_{15}−C_{14} bond, which is adjacent to the protonated Schiff base. The positive bands at 1763 cm^{-1} in H_2O and 1750 cm^{-1} in D_2O can be assigned to the C═O of Asp85, and the ∼13 cm^{-1} difference in frequency from H_2O to D_2O is due to the isotope effect (O═C−OH vs O═C−OD). The appearance of this band is characteristic of the formation of the M intermediate.

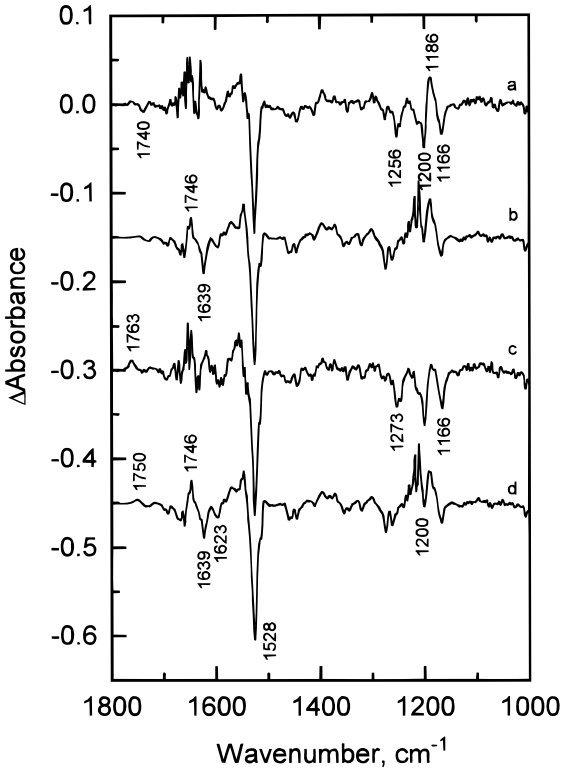

Figure 1. Time-resolved FTIR difference spectra of bR in H_2O and D_2O at room temperature. The spectra are taken at the delay time of 8 μs (L/bR, spectrum a for H_2O and spectrum b for D_2O) and 100 μs (M/bR, spectrum c for H_2O and spectrum d for D_2O). The spectra are vertically shifted with real scale shown.

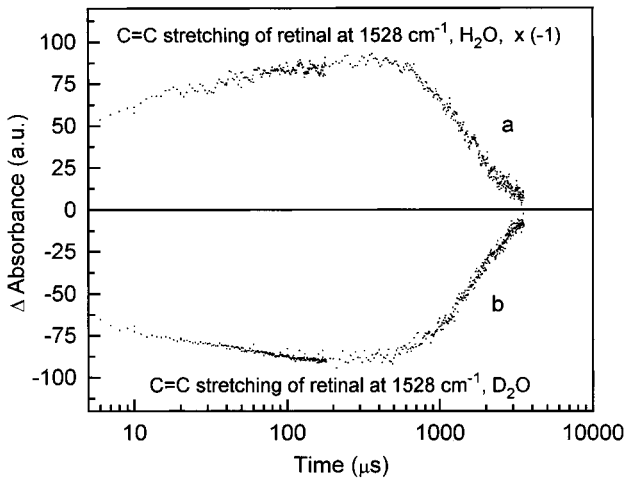

Figure 2. Kinetics of retinal C═C stretching vibrational mode at 1528 cm^{-1}, as an indicator of the photocycle, in the case of H_2O (a) and D_2O (b). Two traces are overlapped for each case, by using time resolution of 1 and 10 μs. Note that there is a minus sign of the absorbance change, in the case of H_2O.

Time Courses of C═C Vibration at 1528 cm^{-1} in H_2O and D_2O. Figure 2 shows the kinetics of the bleach due to the C═C retinal stretching vibrational mode at 1528 cm^{-1}, as an indicator of the photocycle, in H_2O (Figure 2a) and in D_2O (Figure 2b). The decrease in its intensity as a function of time reflects the all-trans to 13-cis retinal isomerization. The photoisomerization process is known to take place in <3ps,[17,18] with the formation of the K intermediate. Because we use 1 μs and/or 10 μs time resolution here, and the MCT detector has a 10

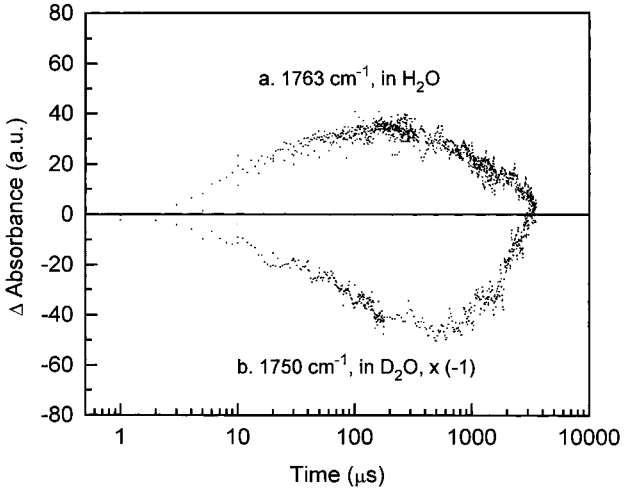

Figure 3. Time courses of the C═O formation/decay of Asp85 from COO^- in the medium of H_2O for protonation/deprotonation processes (a) and in comparison with the deuteronation/dedeuteronation processes in the medium of D_2O (b).

ns response time, the formation and decay of the K intermediate could not be resolved in our time-resolved FTIR experiment. However, the maximum bleach is found to occur at ~500−600 μs, which is due to changes in the retinal planarity and the surrounding protein environment relation following the photoisomerization process. After that, a recovery process begins, corresponding to the relaxation process of the protein and the retinal reisomerization process from the 13-cis to the all-trans bR ground state.

Comparing the time-resolved results in H_2O and in D_2O, we conclude that the overall kinetics of the photocycle as monitored by changes in the C═C retinal stretching vibration seems to be similar.

Kinetics of Asp85 Protonation/Deprotonation and that of the Continuum Absorbance in H_2O and D_2O. Figure 3 shows the time dependence of the protonation/deprotonation process of Asp85 in H_2O (curve a), in comparison with the deuteronation /dedeuteronation process of Asp85 in D_2O (curve b), by monitoring the C═O stretching band that originates from the protonation or deuteronation of the Asp85 COO^- group. This gives the vibrational band located at 1763 and 1750 cm^{-1} respectively. The frequency of COO^- is located at ~1400 cm^{-1} in bR ground state.[19,20] Therefore, a significant blue shift is observed after the proton or deuteron is transferred from the Schiff base to Asp85 COO^-. It can be seen that in the case of D_2O, the formation of COOD, is relatively slower than the formation of COOH in H_2O (Figure 3).

Figure 4 shows the time dependence of the protonation/deprotonation process of Asp85 in H_2O (curve a), in comparison with the broad continuum absorbance integrated between 1850 and 1800 cm^{-1} in H_2O (curve b), and D_2O (curve c). The following are our observations: (a) The protonation process of Asp85 occurs with rise times of 9.7 ± 1.0 μs (26%) and 56.5 ± 3.6 μs (74%), as summarized from several independent measurements (Table 1). These values are in reasonable agreement with the lifetimes of M formation measured from the change in the visible absorption, 12 μs for the fast component and ~71 μs for the slow component.[21] (b) The bleaching process of the integrated continuum band at 1850−1800 cm^{-1} has a rise time of 58.7± 4.8 μs (Table 1), which is in the same order of the rise of the Asp85 C═O infrared absorption. (c) The deprotonation process decays with a time constant of ~2.3 ms, whereas the bleach recovery process of the continuum band at

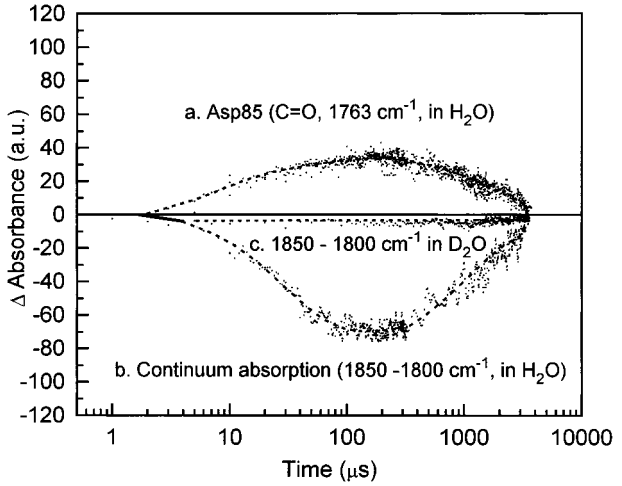

Figure 4. Time courses of the protonation/deprotonation process of COO^- of Asp85 (a) in comparison with the broad continuum absorbance averaged between 1850 and 1800 cm^{-1}, in H_2O (b), and in D_2O (c). The obtained lifetimes for protonation/deprotonation process of Asp85 are 9.7 ± 1.0 μs (26%) and 56.5 ± 3.6 μs (74%) for the protonation and ~2.3 ms for the deprotonation. The obtained lifetimes for the observed bleach continuum band at 1850−1800 cm^{-1} are 58.7 ± 4.8 μs for the formation and ~1.1 ms for the recovery.

TABLE 1. Time Constants and Amplitudes Resulting from Single- or Double-Exponential Fitting to the Time Courses of the C═O Formation of Asp85 and that of the Integrated Band from 1850 to 1800 cm^{-1} in bR/H_2O[a]

	lifetimes and amplitudes for C═O rise at 1763 cm^{-1}		lifetime for the continuum bleach band at 1850−1800 cm^{-1}
exp	τ_{fast} (A_{fast})	τ_{slow} (A_{slow})	τ
1	12.79 (28%)	56.68 (72%)	76.47
2	11.66 (33%)	60.99 (67%)	43.71
3	7.22 (22%)	52.33 (78%)	60.06
4	5.96 (27%)	49.19 (73%)	64.66
5	8.58 (29%)	41.59 (71%)	56.13
6	12.44 (23%)	66.84 (77%)	41.98
7	9.26 (19%)	68.30 (81%)	68.04
avg	9.7 (26%)	56.5 (74%)	58.7
SE (±)	1.0	3.6	4.8

[a] See Figure 4. The averaged values and their statistics are given at the end of Table.

1850−1800 cm^{-1} has a lifetime of 1.1 ms. (e) There is no significant continuum absorption features in the same frequency region (1850−1800 cm^{-1}) in D_2O as a solvent (curve c).

It can be seen that in the case of H_2O, the continuum band decrease is in line with the protonation process of Asp85. Because a previous report[14] has pointed out that the continuum absorbance change in the frequency region of 1900−1800 cm^{-1} is due to the disappearance of a delocalized proton, the similarity of the kinetics of this band and that of the C═O of Asp85 suggests that, during the protonation process of the proton acceptor, Asp85, there is a proton displacement along the H-bonded network occurring at the same time.

If the bleach in the 1850−1800 cm^{-1} is due to a delocalized proton, it should shift to lower frequency in D_2O. We have examined the same frequency region (1850−1800 cm^{-1}), as shown in curve c in Figure 4. Indeed, the continuum band observed in H_2O at 1850−1800 cm^{-1} is no longer present in D_2O. We also examined the spectral change in the frequency region of 1300−1250 cm^{-1}, in which the possible hydrogen/deuterium (H/D) isotopic effect is expected. However, because there are protein fingerprints and retinal C−C stretch mode in

this frequency region, the contribution from the possible continuum absorption due to the delocalized deuteron is hard to be identified. Furthermore, the intensity of the continuum band in the D-bonded network is expected to be weaker due to the fact that the deuteron polarizability resulting from the collective deuteron motion is smaller than that of the proton.[22] This makes the continuum absorption less obvious in the case of D_2O. However, the disappearance of the continuum absorption band in the frequency region of 1850−1800 cm^{-1} in D_2O is the most direct evidence that there is a shift of such a proton motion resulting in the continuum band, as shown in Figure 4c.

Discussion

Protonation/Deprotonation Kinetics of the Proton Acceptor, Asp85. Certain carboxylic acid groups, such as Asp85 and Asp 96, are important because they are directly involved in the proton pumping pathway. On the basis of mutant studies, the assignment of the proton acceptor and proton donator has been very successful.[7,23] It is expected that the transient FTIR spectral changes, which correspond to the protonation and deprotonation process of these groups, may be seen and that they correspond to the local environment change during the photocycle.[7]

From L to M transition, it can be seen that two C═O bands are shown, located at 1740 and 1763 cm^{-1}, in H_2O (Figure 1). These two bands have different origins. The negative band at 1740 cm^{-1} has been reported to have a rise time of 300 ns[17] and can be attributed to the C═O stretching of Asp96 and Asp115. Its intensity increases as the L intermediate is formed.[24] The formation of the negative band at 1740 cm^{-1} in Figure 1 can be used as an indicator for the KL to L transition (Figure 1). Because this is a protein band, this observation might support the assignment of the KL intermediate as a protein state,[17,25] rather than a retinal state.[26,27] On the other hand, the positive band at 1763 cm^{-1} belongs to the C═O stretching mode of Asp85, the appearance and disappearance of this band indicates the protonation and deprotonation processes of the carboxylate group of Asp85.

The present research is focused on the study of the proton transfer from the protonted Schiff base to the proton acceptor Asp85 and the proton release to the extracellular surface. It is believed that the in the L to M transition, the proton is released. However, this proton[12,13] is not the proton that is transferred between the protonated Schiff base and Asp85. This was concluded from the fact that Asp85 remains protonated (a band at 1750 cm^{-1}, Figure 1) after the proton is transferred to the surface in about 50 μs. This "two different proton" mystery has not been solved yet. It suggests that there is another proton donor XH that donates its proton to the surface after Asp85 is protonated.

Continuum Absorbance Change and the H-bonded Network. The H-bonded network in bR is proposed to be involved in the proton-transfer mechanism. This H-bonded network is composed of internal water molecules and amino acid residues. Theoretical study has proposed a model that requires several water molecules in the proton-conducing channel, based on molecular dynamic calculations.[28−30] The original crystal structural model of Henderson allows the presence of water in both extracellular and cytoplasmic half channel.[31] A number of studies have pointed toward a conclusion, with more certainty, that one or more water molecules are near the binding site of retinal Schiff base, and one of them is H-bonded directly to the protonated Schiff base linkage.[32] A neutron diffraction study reveled the presence of four tightly bound water molecules close to the chromophore-binding site of bR.[33] The H/D exchange, followed by a resonance Raman technique, also suggested the presence of structural water molecules at the retinal binding site.[34] FTIR difference spectra have also been used to elucidate the internal water molecules.[35−37] At least one water molecule located near the active site undergoes an increase in the strength of the H-bonding during the bR−K photoreaction.[35] A water molecule with its O−H weakly bound to Asp85, forms stronger H-bonding upon L formation.[36,37]

The early work by Zundel and co-workers suggested that H-bonded network plays a very important role in the proton conduction pathway in bR.[38,39,15] A recent work by Gerwert and co-workers, using room-temperature step-scan time-resolved FTIR,[14] has shown that the continuum band bleach appears and recovers in a comparable time domain as that of a proton release to the extracelluar surface probed by a pH-indicator dye, flourescein.[10,11] These authors suggest that the functional H-bonded network is spanned between the Schiff base and the protein extracellular surface. Their results indicate that during the L to M transition, an H-bonded network release a proton to the extracellular surface of bR. These authors also suggest that it is very unlikely that the Glu204 acts as the proton release group XH, as was previously suggested,[3,13] although Glu204 is suggested to be involved in the H-bonded network.

Because the observed continuum band bleach has similar kinetics as the Asp85 C═O stretching band in our study, it seems that during L to M transition, H-bonded network plays a role in proton transfer. The continuum band bleach occurs as M is being formed, with their lifetimes both in the order of ~50 μs. It is also possible that the continuum band bleach recovery in H_2O synchronizes with the deprotonation process of Asp85 C═O because they have very similar decay time constant as shown in Figure 4. Our results suggest, therefore, that the two independent processes, the transfer of a proton from the Schiff base to Asp85 (which is monitored by the C═O formation at 1763 cm^{-1}) and the release of a different proton to the extracellular surface (which is monitored by the disappearance of the continuum band at 1850−1800 cm^{-1}), are closely coupled events, within experimental errors (see Table 1). This suggests that Asp85 itself might participate in the H-bonded network. Further, it is quite possible that the carboxyl group in Asp85 works as a triggering group for the H-bonded network and, therefore, regulates the proton-transfer pathway.

Acknowledgment. This work was supported by the Department of Energy, Office of Basic Energy Science, Grant No. DE-FG02-97ER14799. We thank Mr. C. Heyes for his assistance in the time-resolved FTIR experiment.

References and Notes

(1) Oesterhelt, D.; Stoeckenius, W. *Methods Enzymol.* **1974**, *31*, 667.
(2) Racker, E.; Stoeckenius, W. *J. Biol. Chem.* **1974**, *249*, 662.
(3) Henderson, R.; Baldwin, J. M.; Ceska, T. A.; Zemlin, F.; Beckmann, E.; Downing, K. H. *J. Mol. Biol.* **1990**, *213*, 899.
(4) Lozier, R. H.; Niederberger, W.; Bogomolni, R. A.; Hwang, S. B.; Stoeckenius, W. *Biochim. Biophys. Acta* **1976**, *440*, 545.
(5) Birge, R. R. *Annu. Rev. Biophys. Bioeng* **1981**, *10*, 315.
(6) Mathies, R. A.; Lin, S. W.; Ames, J. B.; Pollard, W. T. *Annu. Rev. Biophys. Biophys. Chem.* **1991**, *20*, 491.
(7) Braiman, M. S.; Mogi, T.; Marti, T.; Stern, L. J.; Khorana, H. G.; Rothschild, K. J. *Biochemistry* **1988**, *27*, 8516.
(8) Tittor, J.; Soell, C.; Oesterhelt, D.; Butt, H. J.; Bamberg, E. *EMBO J.* **1989**, *8*, 3477.
(9) Otto, H.; Marti, T.; Holz, M.; Mogi, T.; Lindau, M.; Khorana, H. G.; Heyn, M. P. *Proc. Natl. Acad. Sci. U.S.A.* **1989**, *86*, 9228.
(10) Heberle, J.; Dencher, N. A. *Proc. Natl. Acad. Sci. U.S.A.* **1992**, *89*, 5996.

(11) Alexiev, U.; Mollaaghababa, R.; Scherrer, P.; Khorana, H. G.; Heyn, M. P. *Proc. Natl. Acad. Sci. U.S.A.* **1995**, *92*, 372.
(12) Brown, L. S.; Sasaki, J.; Kandori, H.; Maeda, A.; Needleman, R.; Lanyi, J. K. *J. Biol. Chem.* **1995**, *270*, 27 122.
(13) Grigorieff, N.; Ceska, T. A.; Downing, K. H.; Baldwin, J. M.; Henderson, R. *J. Mol. Biol.* **1996**, *259*, 393.
(14) Rammelsberg, R.; Huhn, G.; Luebben, M.; Gerwert, K. *Biochemistry* **1998**, *37*, 5001.
(15) Zundel, G. *J. Mol. Struct.* **1994**, *322*, 33.
(16) Wang, J.-P.; El-Sayed, M. A. *Biophys. J.* **1999**, *76*, 2777.
(17) Wolfgang, H.; Munsok, K.; Frei, H.; Mathies, R. A. *J. Phys. Chem.* **1996**, *100*, 16026.
(18) Atkinson, G. H.; Ujj, L.; Zhou, Y. *J. Phys. Chem.* **2000**, in press.
(19) Maeda, A.; Sasaki, J.; Shichida, Y.; Yoshizawa, T.; Chang, M.; Ni, B.; Needleman, R.; Lanyi, J. K. *Biochemistry* **1992**, *31*, 4684.
(20) Sasaki, J.; Lanyi, J. K.; Needleman, R.; Yoshizawa, T.; Maeda, A. *Biochemistry* **1994**, *33*, 3178.
(21) Lin, G. C.; El-Sayed, M. A.; Marti, T.; Stern, L. J.; Mogi, T.; Khorana, H. G. *Biophys. J.* **1991**, *60*, 172.
(22) Bartl, F.; Deckers-Hebestreit, G.; Altendorf, K.; Zundel, G. *Biophys. J.* **1995**, *68*, 104.
(23) Gerwert, K.; Hess, B.; Soppa, J.; Oesterhelt, D. *Proc. Natl. Acad. Sci. U.S.A.* **1989**, *86*, 4943.
(24) Braiman, M. S.; Bousche, O.; Rothschild, K. J. *Proc. Natl. Acad. Sci. U.S.A.* **1991**, *88*, 2388.
(25) Rödig, C.; Chizhov, I.; Weidlich, O.; Siebert, F. *Biophys. J.* **1999**, *76*, 2687.
(26) Bazhenov, V.; Schmidt, P.; Atkinson, G. H. *Biophys. J.* **1992**, *61*, 1630.
(27) Weidlich, O.; Ujj, L.; Jager, F.; Atkinson, G. H. *Biophys. J.* **1997**, *72*, 2329.
(28) Humphrey, W.; Logunov, I.; Schulten, K.; Sheves, M. *Biochemistry* **1994**, *33*, 3668.
(29) Humphrey, W.; Bamberg, E.; Schulten, K. *Biophys. J.* **1997**, *72*, 1347.
(30) Logunov, I.; Humphrey, W.; Schulten, K.; Sheves, M. *Biophys. J.* **1995**, *68*, 1270.
(31) Henderson, R.; Schertler, F. R. S.; Schertler, G. F. X. *Philos. Trans. R. Soc. London, Ser. B* **1990**, *326*, 379.
(32) Hildebrandt, P.; Stockburger, M. *Biochemistry* **1984**, *23*, 5539.
(33) Papadopoulos, G.; Dencher, N. A.; Zaccai, G.; Bualdt, G. *J. Mol. Biol.* **1990**, *214*, 15.
(34) Deng, H.; Huang, L.; Callender, R.; Ebrey, T. *Biophys. J.* **1994**, *66*, 1129.
(35) Fischer, W. B.; Sonar, S.; Marti, T.; Khorana, H. G.; Rothschild, K. J. *Biochemistry* **1994**, *33*, 12757.
(36) Maeda, A.; Sasaki, J.; Shichida, Y.; Yoshizawa, T. *Biochemistry* **1992**, *31*, 462.
(37) Maeda, A.; Sasaki, J.; Yamazaki, Y.; Needleman, R.; Lanyi, J. K. *Biochemistry* **1994**, *33*, 1713.
(38) Olejnik, J.; Brzezinski, B.; Zundel, G. *J. Mol. Struct.* **1992**, *271*, 157.
(39) Fritsch, J.; Zundel, G.; Hayd, A.; Maurer, M. *Chem. Phys. Lett.* **1984**, *107*, 65.